LBNL-40145
UC-413

CONF-970271--1

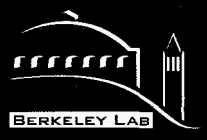

ERNEST ORLANDO LAWRENCE
BERKELEY NATIONAL LABORATORY

Interpreting Multiplicity-Gated Fragment Distributions from Heavy-Ion Collisions

L. Phair, L.G. Moretto, Th. Rubehn, G.J. Wozniak,
L. Beaulieu, N. Colonna, R. Ghetti, and K. Tso
Nuclear Science Division

February1997
Invited paper
presented at the
13th Winter Workshop on Nuclear Dynamics,
Marathon, FL,
February 1–8, 1997,
and to be published in
the Proceedings

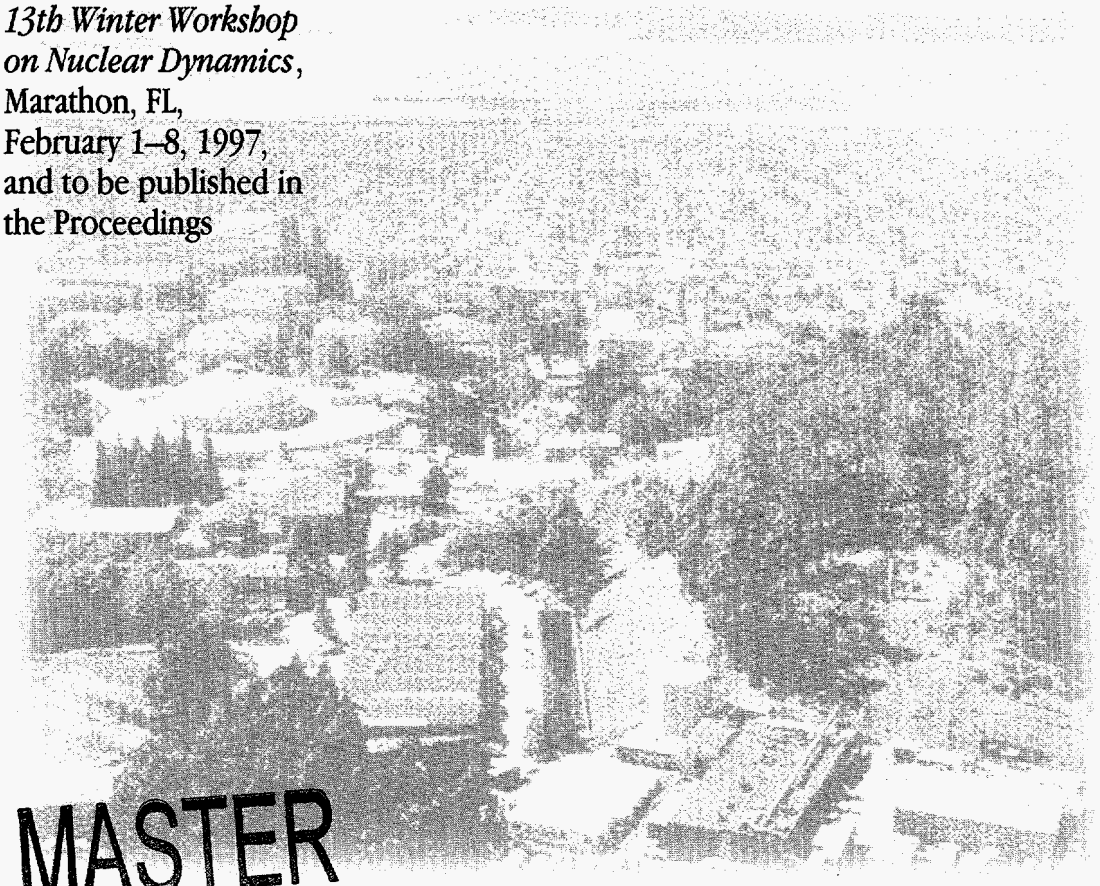

LBNL-40145
UC-413

Interpreting Multiplicity-Gated Fragment Distributions from Heavy-Ion Collisions

L. Phair, L.G. Moretto, Th. Rubehn, G.J. Wozniak, L. Beaulieu,
N. Colonna, R. Ghetti, and K. Tso

Nuclear Science Division
Ernest Orlando Lawrence Berkeley National Laboratory
University of California
Berkeley, California 94720

February 1997

This work was supported in part by the Director, Office of Energy Research, Office of High Energy and Nuclear Physics, Division of High Energy Physics, of the U.S. Department of Energy under Contract No. DE-AC03-76SF00098, and the National Science Foundation under Grant Nos. PHY-8913815, PHY-90117077, and PHY-9214992.

INTERPRETING MULTIPLICITY-GATED FRAGMENT DISTRIBUTIONS FROM HEAVY-ION COLLISIONS

L. Phair, L.G. Moretto, Th. Rubehn, G.J. Wozniak,
L. Beaulieu, N. Colonna*, R. Ghetti†, and K. Tso,

Nuclear Science Division
Lawrence Berkeley National Laboratory, Berkeley, CA

INTRODUCTION

In recent years, multifragmentation of nuclear systems has been extensively studied, and many efforts have been made to clarify the underlying physics[1]. However, no clear consensus exists on the mechanism for multifragmentation. Is the emission of intermediate mass fragments (IMF: $3 \leq Z \leq 20$) a dynamical process (brought on by the occurrence of instabilities of one form or another) or a statistical process (i.e. the decay probabilities are proportional to a suitably defined exit channel phase space)?

Historically the charge (mass) distribution has played and still plays a very important role in characterizing multifragmentation. Since this subject's inception, the near power-law shape of the charge and mass distributions was considered an indication of criticality for the hot nuclear fluid produced in light ion and heavy ion collisions [2, 3]. More modern studies still infer critical behavior from the moments of the charge distribution [4, 5, 6, 7; 8, 9]. Furthermore, a charge distribution is readily predicted by most models and easily compared with data.

In what follows, we point out what the charge distributions might reveal regarding the mechanism of multifragmentation.

STATISTICAL SIGNATURES

Recently, it has been experimentally observed in many heavy-ion reactions that for any value of the transverse energy E_t ($E_t = \sum E_i \sin^2\theta_i$ where E_i and θ_i are the kinetic energy and polar angle of charged particle i in an event), the n-fragment emis-

*INFN-Sez. di Bari, 70126 Bari, Italy.
†Department of Physics, Lund University, Sweden

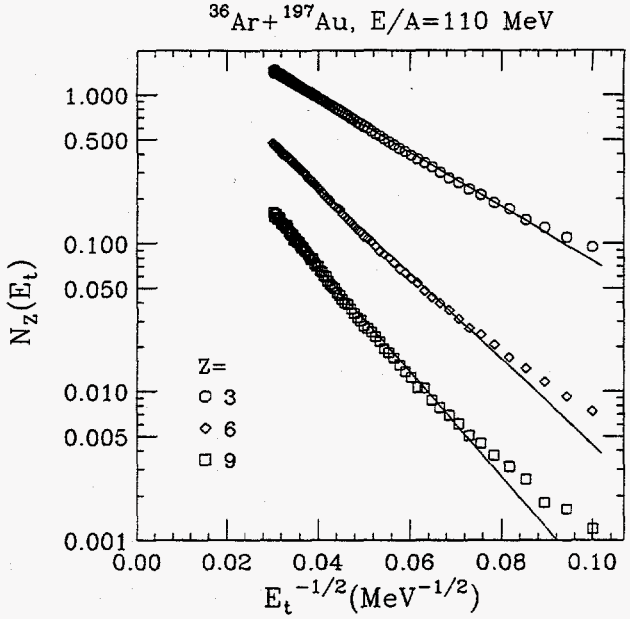

Figure 1. The average yield per event of lithium (circles), carbon (diamonds), and fluorine (squares) as a function of $1/\sqrt{E_t}$. The lines are linear fits to the data.

sion probability P_n is reducible to the one-fragment emission probability p through a binomial distribution [10, 11, 12]

$$P_n^m = \frac{m!}{n!(m-n)!} p^n (1-p)^{m-n}. \tag{2}$$

This empirical evidence indicates that multifragmentation can be thought of as a special combination of nearly independent fragment emissions. The binomial combination of the elementary probabilities points to a combinatorial structure associated with a time-like or space-like one-dimensional sequence [12]. It was also found that the log of such one-fragment emission probabilities ($\log p$) plotted vs $1/\sqrt{E_t}$ (Arrhenius plot) gives a remarkably straight line. This linear dependence is strongly suggestive of a thermal nature for p,

$$p = e^{-B/T} \tag{3}$$

under the assumption that the temperature $T \propto \sqrt{E^*} \propto \sqrt{E_t}$ where E^* is the excitation energy. These observations were made with data integrated over a broad range of fragment atomic numbers ($3 \leq Z \leq 20$). The difficulty of a thermal interpretation of the probability p averaged over Z was tentatively resolved by observing that if B is weakly (polynomial) dependent on Z then

$$p = \int e^{-\frac{1}{T}(B_0 + aZ^s)} dZ = \left(\frac{T}{a}\right)^{1/s} e^{-\frac{B_0}{T}} \tag{4}$$

and therefore p retains the form of Eq. (3).

These aspects of reducibility and thermal scaling in the integrated fragment emission probabilities lead naturally to the question: Is the charge distribution itself reducible and scalable?

By limiting our study to a single value of Z, the emission probabilities become small. The binomial distribution reduces to a Poisson distribution. The observed

average multiplicity is now experimentally equal to the variance. Thus we are in the Poisson reducibility regime and we can check the thermal scaling directly on $\langle n \rangle$. If the charge distributions show "thermal" scaling then the average yield of a given charge should have a Boltzmann form,

$$N_Z \propto e^{-B_Z/T}, \tag{5}$$

where N_Z is the average yield of a given charge Z and B_Z is the Z dependent barrier. For a Poisson distribution $\log N_Z$ should scale linearly then with $1/\sqrt{E_t}$. This can be seen experimentally for the average yield of individual elements of a given charge (see Fig. 1) for the reaction ^{36}Ar+^{197}Au at E/A=110 MeV. In this case of isolating a single species, the reducibility is Poisson, and the thermal (linear) scaling with $1/\sqrt{E_t}$ is readily apparent.

The thermal nature of the charge distributions of this particular data set has been addressed before [13]. In its broadest form, reducibility demands that the probability $p(Z)$, from which an event of n fragments is generated by m trials, is the same at every step of extraction. The consequence of this extreme reducibility is straightforward: the probability distribution for IMF charges emitted from the one-fold events is the same as that for the n-fold events and equal to the singles distributions, i.e.,

$$P_{(1)}(Z) = P_{(n)}(Z) = P_{singles}(Z) = p(Z). \tag{6}$$

If the one-fold = n-fold = singles distributions is thermal, then

$$P(Z) \propto e^{-\frac{B(Z)}{T}} \tag{7}$$

or $T \ln P(Z) \propto -B(Z)$. This suggests that, under the assumption $E_t \propto E^*$ [10, 11, 12, 13, 14], the function

$$\sqrt{E_t} \ln P(Z) = D(Z) \tag{8}$$

should be independent of E_t.

In particular, since the charge distributions (i.e. the probability $P_n(Z)$ to emit an IMF of a given charge Z and a given IMF multiplicity) are exponential,

$$P_n(Z) \propto e^{-\alpha_n Z}, \tag{9}$$

we would expect for α_n the following simple dependence

$$\alpha_n \propto \frac{1}{T} \propto \frac{1}{\sqrt{E_t}} \tag{10}$$

for all folds n. Thus a plot of α_n vs $1/\sqrt{E_t}$ should give nearly straight lines. This is shown in Fig. 2 for ^{36}Ar+^{197}Au at E/A=110 MeV.

The expectation of thermal scaling appears to be met quite satisfactorily. For each value of n the exponent α_n shows the linear dependence on $1/\sqrt{E_t}$ anticipated in Eq. (10). On the other hand, the extreme reducibility condition demanded by Eq. (6), namely that $\alpha_1 = \alpha_2 = ... = \alpha_n = \alpha$, is not met. Rather than collapsing on a single straight line, the values of α_n for the different fragment multiplicities are offset one with respect to another by what appears to be a constant quantity.

In fact, one can fit all of the data remarkably well, assuming for α_n the form

$$\alpha_n = \frac{K'}{\sqrt{E_t}} + nc \tag{11}$$

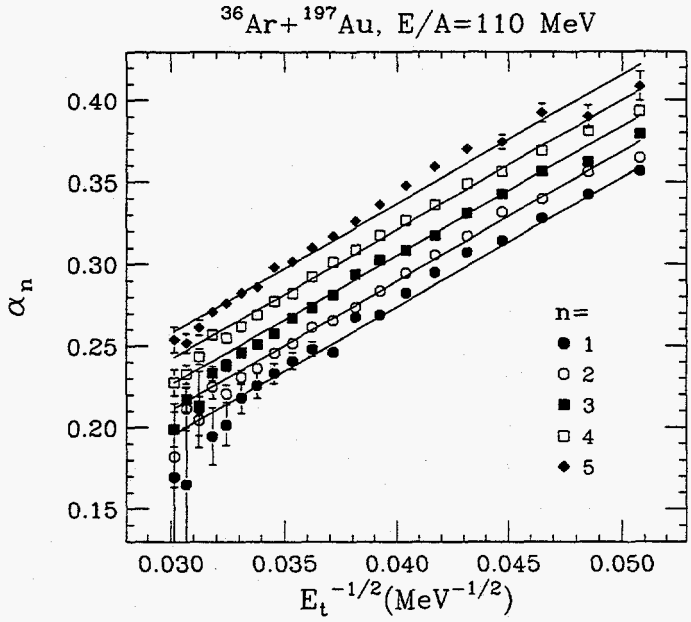

Figure 2. The exponential fit parameter α_n (from fits to the charge distributions, see Eq. (9)) is plotted as a function of $1/\sqrt{E_t}$. The solid lines are a fit to the values of α_n using Eq. (11).

which implies

$$\alpha_n = \frac{K}{T} + nc \tag{12}$$

or more generally, for the Z distribution

$$P_n(Z) \propto e^{-\frac{B(Z)}{T} - ncZ}. \tag{13}$$

Thus, we expect a more general reducibility expression for the charge distribution of any form to be

$$[\ln P_n(Z) + ncZ]\sqrt{E_t} = F(Z) \tag{14}$$

for all values of n and E_t. This equation indicates that it is possible to reduce the charge distributions associated with any intermediate mass fragment multiplicity to the charge distribution of the singles [13].

We stress that the reduced quantity in Eq. (14) is *independent* of the functional form of the charge distribution. However, we have used the fact that the charge distributions are well described by exponential fits in the ^{36}Ar+^{197}Au reaction to summarize the reducibility of an enormous amount of data. Nearly one hundred different charge distributions are represented in Fig. 2.

The origin of the regular offset c has been addressed elsewhere [12, 13, 15, 16].

DYNAMICAL SIGNATURES

It has also been suggested that fragment production might be related to the occurrence of instabilities in the intermediate system produced by heavy ion collisions [17, 18, 19, 20, 21, 22, 23, 24, 25, 26, 27, 28]. In particular, two kinds of instabilities are extensively discussed in the literature: volume instabilities of a spinodal type (see e.g. Ref. [27]) and surface instabilities [18]. Spinodal instabilities are associated with the transit of a homogeneous fluid across a domain of negative pressure, where

the homogeneous fluid becomes unstable and breaks up into droplets of denser liquid. Surface instabilities can be subdivided into Rayleigh or cylinder instabilities which are responsible for the decay of shapes like long necks or toroids [17], and sheet instabilities which cause the decay of bubbles or disklike structures [18]. Many models predict the formation of these exotic geometries which may develop after the initial compression of nuclei in the early stage of the collision for both symmetric and asymmetric systems [18, 19, 21, 22, 25, 26, 27, 28]. Although the scenarios and the models vary, breakup into several *nearly equal-sized* fragments has been discussed for both kinds of instabilities [29]. We have examined model independent signatures that would indicate decay into a number of nearly equal-sized fragments by investigating charge correlations from both experimental data and simulations [30].

We have experimentally studied the reactions Xe+Cu at E/A=50 MeV. The measurements were performed at the National Superconducting Cyclotron Laboratory of Michigan State University using the Miniball [31] and a Si-Si(Li)-plastic forward array [32]. Detailed information on the experiment can be found in Ref. [33].

For comparison, and to determine the sensitivity of our analysis, Monte Carlo calculations have been performed. The created events obey two conditions: the sum charge of all fragments is conserved within an adjustable accuracy, and a fragment is produced according to the probability resulting from the experimental finding, that the charge distributions for n intermediate mass fragments are nearly exponential functions [13],

$$P_n(Z) \propto \exp(-\alpha_n Z). \tag{15}$$

In our simulations, we have chosen $\alpha_n = 0.3$ (different values between 0.2 and 0.4 do not change our findings). The size of the decaying source ($Z_{source} = 83$) was chosen to be equal to the sum charge of Xe and Cu. Events with N_{IMF} equal sized fragments of charge Z_{art} were randomly added with probability P to simulate a dynamical breakup of the system into nearly equal-sized pieces. Furthermore, the charge distributions of the individual fragments from such events were smeared according to a Gaussian distribution. This smearing of the charge distribution roughly accounts not only for the width of the distribution due to the formation process, but also for the subsequent sequential decay of the primary fragments (i.e. the evaporation of light charged particles). In the following, the full width at half-maximum of this distribution is denoted by ω. We have demanded that at least 75% of the total available charge is emitted according to Eq. (15); i.e. the production of particles was stopped in the simulation once this percentage had been reached. We note that in this simple approach the transverse energy E_t has not been simulated. Furthermore, we restrict our analysis to IMFs only.

We have investigated two-particle correlations. Both the experimental and the simulated events have been analyzed according to the following method. The two-particle charge correlations are defined by the expression

$$\left.\frac{Y(Z_1,Z_2)}{Y'(Z_1,Z_2)}\right|_{E_t,N_{IMF}} = C[1+R(Z_1,Z_2)]|_{E_t,N_{IMF}}\,. \tag{16}$$

Here, $Y(Z_1,Z_2)$ is the coincidence yield of two particles of atomic number Z_1 and Z_2 in an event with N_{IMF} intermediate mass fragments and a transverse energy E_t. The background yield $Y'(Z_1,Z_2)$ is constructed by mixing particle yields from different coincidence events selected by the same cuts on N_{IMF} and E_t. The normalization constant C ensures equal integrated yields of Y and CY'.

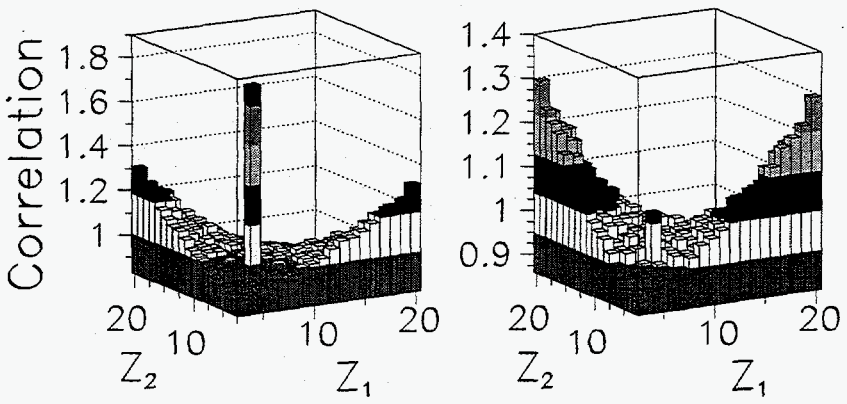

Figure 3. Two-particle charge correlations of IMFs from simulations investigating events with $N_{IMF} = 6$ and a source size of 83. Randomly, 1% (left panel) and 0.1% (right panel) of the events were chosen to have equal sized fragments ($Z_{art} = 6$).

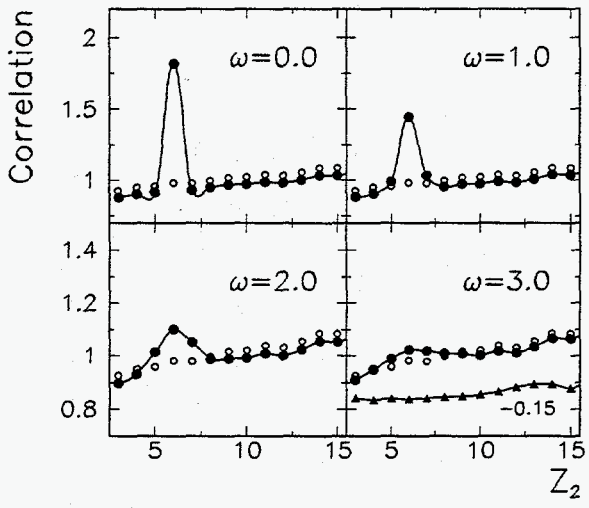

Figure 4. Two-particle charge correlations resulting from simulations for $Z_1 = 6$ as a function of the fragment charge Z_2 for different values of the width of the charge distribution ω. Randomly, 1% of the events were chosen to have nearly equal sized fragments (full circles). For comparison, we have also plotted a calculation where no additional events with equal-sized fragments have been added (open circles). Experimental results for the case $N_{IMF} = 6$ are shown in the right lower panel (full triangles). For clarity, these values are vertically shifted by a value of -0.15. The error bars are smaller than the size of the symbols.

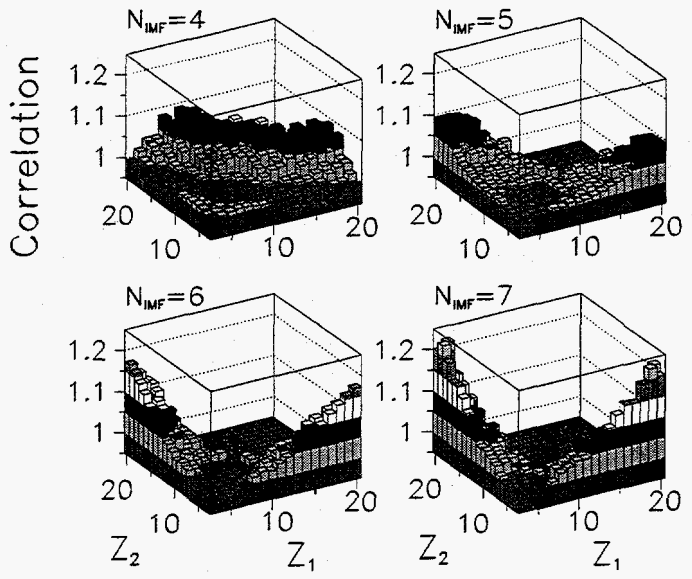

Figure 5. Experimental two-particle charge correlations for the reaction Xe+Cu at E/A=50 MeV. The different figures correspond to N_{IMF} cuts between 4 and 7.

To demonstrate the sensitivity of our method to breakup configurations producing equal-sized fragments, we show in Fig. 3 the results of simulations for the case $N_{IMF} = 6$. Here, a "contamination" of 1% of the events consisting of fragments which all have the size $Z_{art} = 6$ has been added to the data set. The peak produced by these fragments is clearly visible, even if we decrease the yield of equal-sized fragments to only 0.1%. A different choice of Z_{art} does not change our results; higher values would produce an even larger signal since the denominator value is smaller.

The magnitude of the peak shown in Fig. 3 depends not only on the yield, but also on the width of the charge distribution of the nearly equal-sized fragments. In Fig. 4, we show the correlation functions (solid circles) for different widths ω and for $Z_1 = 6$. For comparison, we have plotted the results of a calculation (open circles) where no additional events with equal-sized fragments have been added: As expected, a dependence of the size of the peak on the smearing can be observed which limits the sensitivity of the two-particle correlation functions to an enhancement of events where the charge distribution is relatively narrow. Thus, for possible secondary decay resulting in large values of ω, our analysis might not be adequate. The same analysis used for the simulation has been applied to experimental data. In Fig. 5, we show the results for central collisions (top 5% of events sorted by E_t) of Xe+Cu at E/A=50 MeV for different N_{IMF} cuts. With higher fragment multiplicity the distribution peaked along the line $Z_1 + Z_2 \approx 30$ changes into a distribution peaked at values where one fragment is heavy and its partner is light. However, an enhanced signal for breakup into nearly equal-sized fragments (a signal appearing along the diagonal) was not observed in *any* of the N_{IMF} bins. As an example, we show in Fig. 4 the experimental two-particle correlation function vs. Z_2 for $N_{IMF} = 6$ and $Z_1 = 6$ (triangles).

Furthermore, we have investigated the correlation functions obtained by our simulations without enhanced breakup for several IMF multiplicities. The evolution of the shape of the distribution with increasing values of N_{IMF} is very similar to that observed in the experimental data of Fig. 5. Simulations with different system sizes

show that the charge correlations decrease as Z_{source} increases; this can be attributed to the definition of an IMF ($3 \leq Z_{IMF} \leq 20$) relative to Z_{source}. We have also performed calculations using a percolation code and have observed a dependence similar to that presented in Fig. 5. To further study the evolution of the distributions' shape with multiplicity, we have investigated the breakup of an integer number Z_0 (chain) into n pieces. The calculated two-particle correlation functions for different multiplicities n have an evolution with n similar to that shown in Fig. 5. These findings suggest that the observed experimental evolution of the shape of the two-particle charge correlation distribution with fragment multiplicity may be due to the limited number of possibilities to create fragments if charge is conserved and the number of fragments is fixed. A signal of enhanced emission will sit on top of such a background.

CONCLUSIONS

In conclusion, we have studied different aspects of the charge distributions. The implications of the experimental evidence presented above are potentially far reaching.

On the one hand, the thermal features observed in the n-fragment emission probabilities for the ^{36}Ar+^{197}Au reaction [10] extend consistently to the charge distributions and strengthen the hypothesis of the important role of phase space in describing multifragmentation.

On the other hand, we have investigated charge correlation functions of multifragment decays to search for the enhanced production of nearly equal-sized fragments predicted in several theoretical works. The analysis of experimental data for the reactions Xe+Cu and Xe+Au at E/A=50 MeV and Ar+Au at E/A=50 and 110 MeV, however, shows no evidence for a preferred breakup into nearly equal-sized fragments. Recently, two groups have reported experimental signatures of possible formations of non-compact geometries in the reactions ^{86}Kr on ^{93}Nb at E/A=65 MeV and Pb+Au at E/A=29 MeV, respectively [34, 35]. It would be interesting to analyze these data using the method outlined above.

ACKNOWLEDGEMENTS

This work was supported by the Director, Office of Energy Research, Office of High Energy and Nuclear Physics, Nuclear Physics Division of the US Department of Energy, under contract DE-AC03-76SF00098 and by the National Science Foundation under Grant Nos. PHY-8913815, PHY-90117077, and PHY-9214992.

REFERENCES

1. L.G. Moretto and G.J. Wozniak, Ann. Rev. of Nucl. & Part. Sci., **43**, 379 (1993).
2. J.E. Finn *et al.*, Phys. Rev. Lett. **49**, 1321 (1982).
3. A.D. Panagiotou *et al.*, Phys. Rev. Lett. **52**, 496 (1984).
4. X. Campi, Phys. Lett. **B208**, 351 (1988).
5. W. Bauer, Phys. Rev. **C38**, 1297 (1988).
6. W. Trautmann, U. Milkau, U. Lynen, and J. Pochodzalla, Z. Phys. **A344**, 447 (1993) and refs. therein.
7. T. Li et al., Phys. Rev. Lett. **70**, 1924 (1993).
8. P. Kreutz *et al.*, Nucl. Phys. A **556**, 672 (1993).

9. M. L. Gilkes *et al.*, Phys. Rev. Lett. **73**, 1590 (1994).
10. L.G. Moretto et al., Phys. Rev. Lett. **74**, 1530 (1995).
11. K. Tso *et al.*, Phys. Lett. B **361**, 25 (1995).
12. L.G. Moretto *et al.*, Phys. Rep., in press.
13. L. Phair *et al.*, Phys. Rev. Lett. **75**, 213 (1995).
14. L. Phair *et al.*, Phys. Rev. Lett. **77**, 822 (1996).
15. A. Ferrero *et al.*, Phys. Rev. C **53**, R5 (1996).
16. L.G. Moretto *et al.*, Phys. Rev. Lett. **76**, 372 (1996).
17. U. Brosa, S. Grossmann, A. Müller, and E. Becker, Nucl. Phys. **A 502**, 423c (1989); Phys. Rep. **197**, 167 (1990).
18. L.G. Moretto, K. Tso, N. Colonna, and G.J. Wozniak, Nucl. Phys. **A 545**, 237c (1992); Phys. Rev. Lett. **69**, 1884 (1992).
19. W. Bauer, G.F. Bertsch, and H. Schulz, Phys. Rev. Lett. **69**, 1888 (1992).
20. D.H.E. Gross, B.A. Li, and A.R. DeAngelis, Ann. Physik **1**, 467 (1992).
21. S.R. Souza and C. Ngô, Phys. Rev. C **48**, R2555 (1993).
22. H.M. Xu *et al.*, Phys. Rev. C **48**, 933 (1993).
23. L. Phair, W. Bauer, and C.K. Gelbke, Phys. Lett. **B 314**, 271 (1993).
24. T. Glasmacher, C.K. Gelbke, and S. Pratt, Phys. Lett. **B 314**, 275 (1993).
25. B. Borderie, B. Remaud, M.F. Rivet, and F. Sebille, Phys. Lett. **B 302**, 15 (1993).
26. S. Pal, S.K. Samaddar, A. Das, and J.N. De, Phys. Lett. **B 337**, 14 (1994).
27. Ph. Chomaz, M. Colonna, A. Guanera, and B. Jacquot, Nucl. Phys. **A 583**, 305c (1995).
28. D.O. Handzy *et al.*, Phys. Rev. C **51**, 2237 (1995).
29. M. Bruno *et al.*, Phys. Lett. **B 292**, 251 (1992); Nucl. Phys. **A 576**, 138 (1994).
30. L.G. Moretto *et al.*, Phys. Rev. Lett. **77**, 2634 (1996).
31. R.T. de Souza *et al.*, Nucl. Inst. Meth. **A 311**, 109 (1992).
32. W.C. Kehoe *et al.*, Nucl. Inst. Meth. **A 311**, 258 (1992).
33. D.R. Bowman *et al.*, Phys. Rev. C **46**, 1834 (1992).
34. N.T.B. Stone *et al.*, Phys. Rev. Lett. **78**, 2084 (1997).
35. D. Durand *et al.*, submitted to Phys. Lett. B; J.F. Lecolley *et al.*, submitted to Phys. Lett. B.